Carbon 105 (2016) 305–313

Contents lists available at ScienceDirect

Carbon

journal homepage: www.elsevier.com/locate/carbon

Facile preparation of lightweight high-strength biodegradable polymer/multi-walled carbon nanotubes nanocomposite foams for electromagnetic interference shielding

Tairong Kuang [a, b, 1], Lingqian Chang [b, 1], Feng Chen [b, c], Yan Sheng [b], Dajiong Fu [a, b], Xiangfang Peng [a, *]

[a] National Engineering Research Center of Novel Equipment for Polymer Processing, The Key Laboratory of Polymer Processing Engineering of Ministry of Education, South China University of Technology, Guangzhou, 510640, China
[b] NSEC Center for Affordable Nanoengineering of Polymeric Biomedical Devices, The Ohio State University, Columbus, OH 43210, USA
[c] College of Materials Science and Engineering, Zhejiang University of Technology, Hangzhou, 310014, China

ARTICLE INFO

Article history:
Received 22 February 2016
Received in revised form
12 April 2016
Accepted 22 April 2016
Available online 23 April 2016

ABSTRACT

Lightweight conductive polymer composites (CPCs) have been considered as the most promising alternatives to metal-based shields for electromagnetic interference (EMI) shielding application but still face non-degradation issues. We report a facile, inexpensive and green method to implement lightweight biodegradable poly (L-lactic acid) (PLLA)-multiwalled carbon nanotubes (MWCNTs) nanocomposite foams using a combinatorial technology of pressure-induced flow (PIF) processing and supercritical carbon dioxide (Sc–CO_2) foaming. Such low-density (~0.3 g/cm^3), low thickness (~2.5 mm), high compressive strength (~54 MPa g^{-1} cm^3)) and highly conductive (~3.4 S m^{-1}) PLLA-MWCNT nanocomposite foams were first reported as an EMI shielding material: it presents high performance EMI shielding with a remarkable effectiveness and a corresponding average specific EMI SE of ~23 dB and ~77 dB g^{-1} cm^3, respectively, with less reflection in the measured X-band frequency region. Considering the simple, low-cost and eco-friendly fabrication process, the lightweight, high-strength and highly conductive biodegradable polymer composite foams are expected to be used as high-performance EMI shielding materials in areas such as electronics, automobiles and packaging.

1. Introduction

Electromagnetic interference (EMI) shielding attracts wide attentions in aerospace, electronics, communication and packaging fields, since proper EMI protection would not only ensure the good working of the related electronic devices, but also minimize the radiative damage to human body [1–3]. Till now, metals and polymer composites are the two most common shielding materials. Compare to the conventional metal-based shielding materials, conductive polymer composites (CPCs) containing electric fillers, i.e., graphene, carbon nanotube (CNT), carbon black (CB), carbon nanofiber (CNF), have their intrinsic advantages, such as weight savings, ease of processing, strong resistance against corrosion, low-cost and tunable electric conductivities [4–10]. Nevertheless, CPCs has not yet successfully replaced metal-based shielding materials due to high electric fillers loading in the polymer matrix that caused by the requirement of EMI shielding effectiveness (SE) (≥20 dB). Meanwhile, high contents of fillers lead to poorer mechanical properties and process-ability, higher weight, and other worse performance than CPCs with low loading fillers, especially the weight increment.

Being lightweight is a key technological factor for the practical EMI shielding application [11]. The reduction in the weight of CPCs is particularly desirable. To achieve the low-density EMI materials, foaming not only provide an effective way to decrease the density, and also makes the processing procedure easier while maintaining/improving the performance. Gupta et al. [11] prepared low-density polystyrene (PS)/CNT composite foams using chemical foaming agent, and found that the EMI SE of PS/CNT composite foams was 19 dB for 7wt% CNT loading at a density of 0.56 g/cm^3. Zheng et al. [12] also fabricated lightweight microcellular polyetherimide (PEI)/

* Corresponding author.
E-mail address: pmxfpeng@scut.edu.cn (X. Peng).
[1] These authors contributed equally to this work.

http://dx.doi.org/10.1016/j.carbon.2016.04.052
0008-6223/

graphene composite foams by a phase separation process, indicated that achieve a density of ~0.3 g/cm^3 and a corresponding specific EMI SE of 44.1 dB/g·cm^3 at the 10wt% filler loading. Recently, Park et al. [13] used injection molding foaming process to prepare polypropylene (PP)/stainless-steel fiber composite foams with a density of 0.64 g/cm^3 and achieved a EMI SE of 48 dB, corresponding to a specific EMI SE of 75 dB/(g/cm^3). Other polymer systems, such as PMMA [14] and PC [15], have also been studied for EMI shielding. However, most of these CPCs systems were processed based on traditional petrochemical-derived plastics, which would cause serious environmental issues such as fossil fuel consumption, ecological hazards (non-degradable) and carbon dioxide emission concerns, thus limiting the widespread use of those CPCs foams as EMI shielding materials in practical applications.

Given the advantages such as sustainable, renewable resource, and environmental friendly, biodegradable polymers have attracted increasing attentions for replacing the petrochemical based systems in EMI shielding field [16,17]. Recent year, one of the most widely used biodegradable polymers is poly (L-lactic acid) (PLLA), which has gained great interests. It was derived from the renewable source such as corn and sugarcane, and could be fully degraded, as compared to the petrochemicals. PLLA also has extraordinary mechanical strength, easy process-ability, and good thermal plasticity. Thus, it has been considered as a viable candidate to petrochemical-based polymers such as polyethylene terephthalate (PET), polystyrene (PS), polypropylene (PP) and polycarbonate (PC) for many applications (e.g., electronic, packaging, etc.). By far, however, the research on preparation of lightweight PLLA nanocomposite foams for the use of EMI shielding materials was rarely found. The reasons for that is because the intrinsic low melt strength and slow crystallization rate of PLLA matrix makes it harder to obtain low-density (below ~0.3 g/cm^3) and uniform morphology foams; loading carbon-based electric fillers always causes adverse effects for the foamability of composites [18]; thereby restricts it use as a EMI shielding materials in electronics, communication and other special areas.

In this work, we report a facile, efficient, inexpensive and chemical-free fabrication method to produce lightweight and highly conductive biodegradable nanocomposite (PLLA/MWCNT) foams for high-performance EMI shielding. The nanocomposite foams were prepared by using a combined technology of pressure-induced flow processing (PIF) and supercritical CO_2 (Sc–CO_2) foaming. The influences of MWCNTs on the morphology, mechanical property, electric conductivity, and EMI shielding performance of the nanocomposite foams are explored. The EMI shielding mechanisms of the nanocomposite foams are also discussed.

2. Experimental details

2.1. Materials

Poly(L-lactic acid) (PLLA) pellets (2500HP, density: 1.24 g/cm^3, MFR: 8 g/10 min) were purchased from Natureworks LLC (USA) with 4.0 dL/g inherent viscosity. Multi-walled carbon nanotubes (MWCNTs) with a diameter of 10–15 nm and an average length of 0.1–10 μm were purchased by Arkema Inc. (Graphistrength®, US). Commercial carbon dioxide (CO_2), supplied by OSU stores, was used as the physical blowing agent for solid-state foaming.

2.2. Preparation of PLLA/MWCNT nanocomposites with "brick and mud" structure

The PLLA/MWCNT nanocomposites were prepared by a mechanical mixing process, which is similar to the previous work [19]. For a typical perform sample, MWCNTs (0.3–6 g) were mechanically mixed with PLLA pellets (60 g) and ball grinder (150 g) in a high-speed mixers (300 rpm) for 30 min at 110 °C. Then the obtained mixtures were compression molded into a sheet of 80 mm diameter and 3 mm thickness at 210 °C, 10 MPa for 10 min, and the PLLA/MWCNT nanocomposites with a honeycomb-like structure was obtained. The obtained PLLA/MWCNT nanocomposites were cut into a certain rectangle plate size and deformed into a sheet in a designed molded at the temperature of 110 °C, the pressure of 450 MPa for 10 min. During the process, the nanocomposites were forced to deform in one direction and eventually formed the "brick and mud" structure. The above process is called pressure-induced flow (PIF). For convenience, different weight fractions of MWCNTs in the PLLA matrix were named as PLLAC0.5, PLLAC1.0, PLLAC3.0, PLLAC5.0, and PLLAC10.0, respectively.

2.3. Fabrication of lightweight PLLA/MWCNT nanocomposites foams

PLLA/MWCNT nanocomposite foams were prepared using a solid-state supercritical carbon dioxide (Sc–CO_2) process. The as-prepared composites were saturated with Sc–CO_2 in a lab-designed high-pressure apparatus at a temperature of 155 °C and the pressure of 20 MPa for 3 h to achieve full saturation. After the complete saturation, the samples were quickly cooled down to the foaming temperature (120 °C) and were held for 3 min. Then, the pressure was rapidly released in 2–3 s to induce the cell nucleation and bubble growth.

2.4. Characterization

Transmission electron microscopy (TEM) was carried out by a JEOL JEM-1200EX microscope, and operated at an accelerating voltage of 120 kV. The sample with a thickness of approximately 80 nm was micro-tomed at room temperature using a diamond knife. The cross-section microstructure of nanocomposites and foams were observed with a Hitachi S-4300 (Tokyo, Japan) scanning electron microscopy (SEM). Before testing, the sample was coated with a thin gold layer (5 nm). The pore size and pore density were calculated from SEM micrographs by Image-pro Plus software. The pore density (N_o) was determined using equation as follow [20]:

$$N_o = \left(\frac{nM^2}{A}\right)^{\frac{3}{2}} \frac{\rho_{solid}}{\rho_{foam}} \quad (1)$$

where n is the number of cells in the SEM photo, M is the magnification, A is the area of the SEM micrograph (cm^2), and ρ_{solid} and ρ_{foam} are the densities of PLLA/MWCNT nanocomposites before and after foam.

Compression strength test was carried out by a universal testing machine (Instron 5566, USA) at room temperature with a compression speed of 0.5 mm/min. For each average value (Fig. 6), at least four samples were tested independently.

The electrical conductivity of solid and foamed PLLA/MWCNT composites sample was measured using a KEITHLEY series2400 source meter according to the Van der Pauw technique (four-point contact method) [21]. At least four specimens were tested for each sample, and the average value was used in this work (Fig. 6).

EMI SE was measured in the X-band frequency range of 8.00–12.48 GHz by a N5230A PNA-L Network analyzer system with an S-parameter set at room temperature based on ASTM D4935-99 method [22]. The test samples were cut from the foaming samples and sized into the same rectangle shape with a dimension of

25.4 × 12.7 mm^2 (thickness is 2.54 mm) to fit the sample holder. When electromagnetic radiation is incident on the shielding materials, the incident power is divided into reflected power, absorbed power and transmitted power. The absorptivity (A), reflectivity (R) and transmissivity (T) must add up to 1, that is, A + R + T = 1. The reflectance, transmittance and effective absorbance can be expressed as follows [5]:

$$SE_R = -10\log(1-R) \quad (2)$$

$$SE_{total} = -10\log T \quad (3)$$

$$A = 1 - R - T \quad (4)$$

3. Results and discussions

3.1. Morphology and dispersion of MWCNTs in PLLA matrix

The microstructures of PLLA/MWCNT nanocomposites characterized with TEM are shown in Fig. 1. At low MWCNT loadings (0.5 wt%), small amount of MWCNTs are uniformly and separately dispersed in the composites without a conductivity network. As the MWCNTs loadings increase to 10wt%, the MWCNTs were closely covered in the PLLA matrix, forming a strong conductive network, which is beneficial for enhancing the electrical conductivity (discussion is given in Section 3.4).

3.2. Morphology of PLLA/MWCNT nanocomposites before and after PIF

The cross-section microstructures of neat and PIF PLLA/MWCNT nanocomposites are showed in Fig. 2. Clearly, the highly orientated structures were observed after PIF processing, which are essential for fabricating the lightweight foams during Sc–CO_2 foaming process.

3.3. Fabrication of lightweight PLLA/MWCNT nanocomposite foams

The fabrication of lightweight PLLA/MWCNT nanocomposite foams is illustrated in Fig. 3. First, MWCNTs were mechanically mixed with PLLA pellets in a high-speed mixer for 30 min, at a speed of 300 rpm and a temperature of 110 °C. The process was utilized to prepare the honey-comb like PLLA-MWCNT structure, and the MWCNTs were successfully coated on the surface of PLLA pellets [19] Then the obtained pellets were compression molded into the rectangle sheet (3 mm × 12 mm × 25 mm in this case) under a pressure of 20 MPa at 210 °C for 10 min. Subsequently, the obtained coating sample was processing at 110 °C, under a pressure of 450 MPa for PIF processing. After that, the crystal lamellas were forced to deform under the temperature and pressure conditions, which results in highly orientated co-continuous “brick and mud” crystalline structure. During the Sc–CO_2 foaming soaking process, the “brick and mud” structure could improve the melt strength of PLLA and slow down the CO_2 gas diffusion so that more bubbles nucleation and growth are induced.

Table 1 shows the foam density of PLLA/MWCNT nanocomposite foams as a function of MWCNT content. In general, the stiffness of polymer matrix can be increased by the addition of nano-fillers [23], which causes higher weight of polymer composite foams or lightweight with inhomogeneous pore structure. Interestingly, we found that the densities of nanocomposite foams in this work were ranging from 0.18 to 0.30 g/cm^3, which correspond to the MWCNT content ranging from 0.5wt% to 10wt%. Such low-density PLLA-based nanocomposite foams with uniform pore structure were

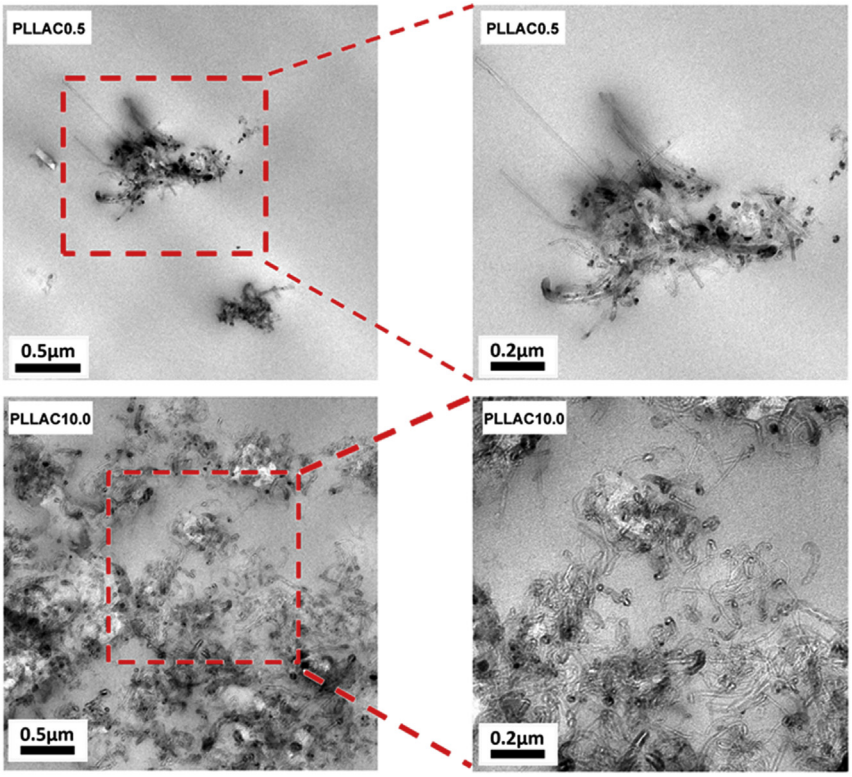

Fig. 1. Representative TEM micrographs for PLLA/MWCNT nanocomposites. (A color version of this figure can be viewed online.).

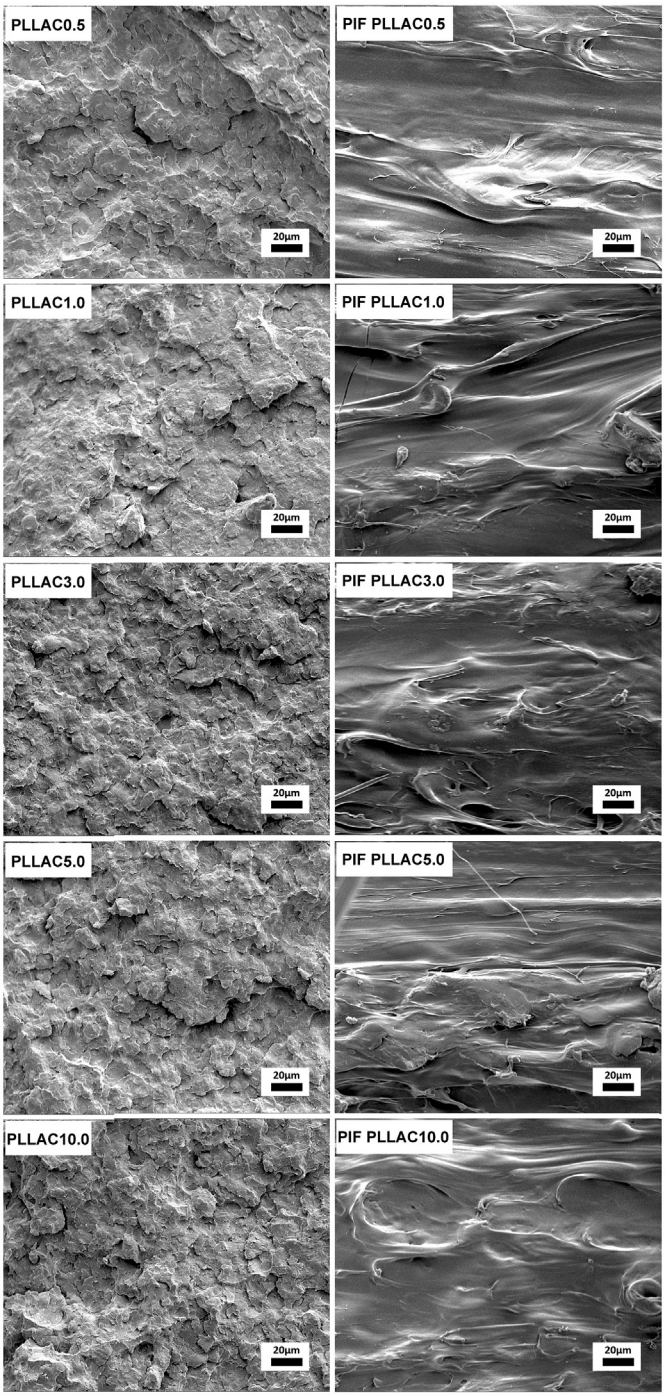

Fig. 2. SEM morphology of PLLA/MWCNT nanocomposites before and after PIF processing.

successfully obtained.

The morphological observation of the PLLA/MWCNT nanocomposite foams with various MWCNT content is presented in Fig. 4. The cell morphology of foams presents uniform foaming behavior, which is attributed to the increased melt strength and slowed down the gas loss by "brick and mud" structure. Compare to the neat PLLA foams, the morphology of nanocomposite foams show the clear changes in the cell shape, size and wall thickness. Fig. 5 displays the average pore sizes and densities of composite foams. The addition of MWCNTs gradually decreased the cell size and increased the cell densities, possibly due to the heterogeneous nucleation effects of MWCNTs in the polymer matrix [24]. Furthermore, such a uniform typical open-cell structure is caused by the accelerated crystallization rate during the Sc–CO_2 foaming process. To our best knowledge, this is the first time to report such low-density and uniform open-cell morphology of PLLA-based biodegradable polymer nanocomposite foams, and these uniform interconnected 3D foam morphologies show beneficial features for the electrical conductivity and EMI SE properties.

3.4. Mechanical property and electric conductivity of PLLA/MWCNT nanocomposites foams

The mechanical properties of the PLLA/MWCNT nanocomposite foams were tested and the representative compressive stress–-strain curves for PLLA/MWCNT nanocomposite foams are presented in Fig. 6a. All of the data for comparison were taken at 40% compressive strain. It is clear that these curves behave as a typical curve for "elastic–plastic" foams [25]. At lowing loadings of MWCNT (1wt%), the compressive stress of nanocomposite foams shows 5 times higher stress than that of neat PLLA foams, even the specific strength (divide compressive stress by density). Further growing MWCNT contents, drastically improve the specific compressive stress, eventually reach a value as high as ~54 MPa/(g/cm^3) with 10wt% MWCNT. Such a compressive stress value 54 MPa/(g/cm^3) is higher than other reported PLLA, PLLA-based and biodegradable polymer composites foams with similar densities in the open literatures [25–27]. These significant improvements of mechanical properties are attributed to the "brick and mud" structure, uniform foam morphology and small cells.

The electrical conductivities of PLLA/MWCNT nanocomposites and foams as a function of MWCNT volume content at room temperature are shown in Fig. 6b. Increasing the MWCNT contents significantly increase the electrical conductivity of the nanocomposites, which is due to the formation of conductive MWCNT networks in the composites (Fig. 1). Note that the composite foams present a much higher conductivity than pure composite at the same MWCNT loadings. For instance, composite foams with 1.47 vol% MWCNT achieved an electrical conductivity of 3.4 S/m, which is three times higher than the conductivity of composites with 5.40 vol% MWCNT, and far surpass the target value of electrical conductivity for commercial EMI shielding materials (1 S/m). These results suggest that the presence of microcellular structure might decrease the percolation threshold of the composite foams.

To further evaluate the relationship between electrical conductivity and MWCNT content, the percolation threshold was predicted quantitatively using power-law behavior [28]:

$$\sigma \propto (\phi - \phi_c)^t \tag{5}$$

where σ is the electrical conductivity of the composite, ϕ is the volume fraction of the MWCNT, ϕ_c is the percolation threshold, and t is the critical exponent. The best fitting results of composites and composite foams are shown in the inset of Fig. 6c. According to the fitting results, the fitted ϕ_c of composite foams is ~0.16 vol%, which is much lower than those of the composite (~0.66 vol%), which confirms that the microcellular pore structure is beneficial to enhance the electrical conductivity of PLLA/MWCNT composites. The optimum fitted t value is 3.13 and 3.45 for composite and composite foams, respectively, which further confirm the formation of 3D MWCNT conductive networks [7,28]. We thus conclude that the reason for the enhanced conductivity of composite foams is that the volume expansion of foam sample induces a significant decrease of the average distance between MWCNTs [29], and the uniform interconnected 3D porous morphologies built a 3D

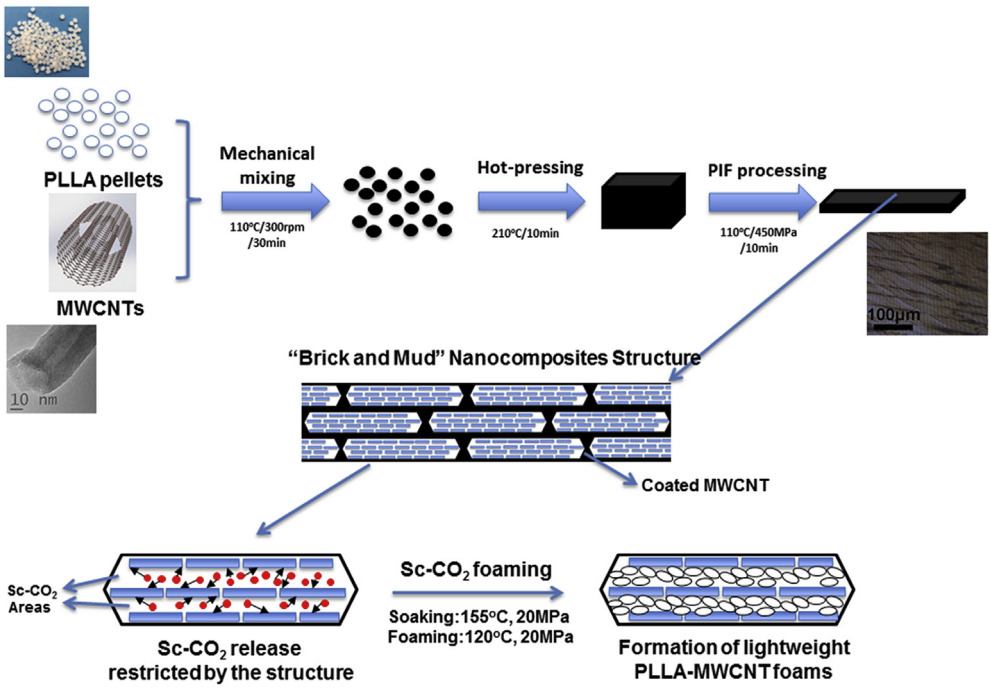

Fig. 3. Schematic of the fabrication of lightweight PLLA/MWCNT nanocomposite foams using a combinatorial technology of PIF processing and Sc–CO_2 foaming. (A color version of this figure can be viewed online.)

Table 1
Processing parameters and Density Values of PLLA-MWCNT Foams with various MWCNT Contents.

MWCNT content in nanocomposites (wt%)	MWCNT content in nanocomposites (initial vol%)	PIF conditions (°C/MPa)	Foam conditions		MWCNT content in foams (vol%)	Foam density[a] (g/cm^{-3})
			Soaking (°C/hours)	Foaming (°C)		
0	0	110/450	155/3	120	0	0.09
0.5	0.29	110/450	155/3	120	0.05	0.18
1.0	0.59	110/450	155/3	120	0.13	0.22
3.0	1.74	110/450	155/3	120	0.42	0.25
5.0	2.83	110/450	155/3	120	0.70	0.28
10.0	5.40	110/450	155/3	120	1.47	0.30

[a] Using water-displacement method (According to ASTM D792-00 standard) [12].

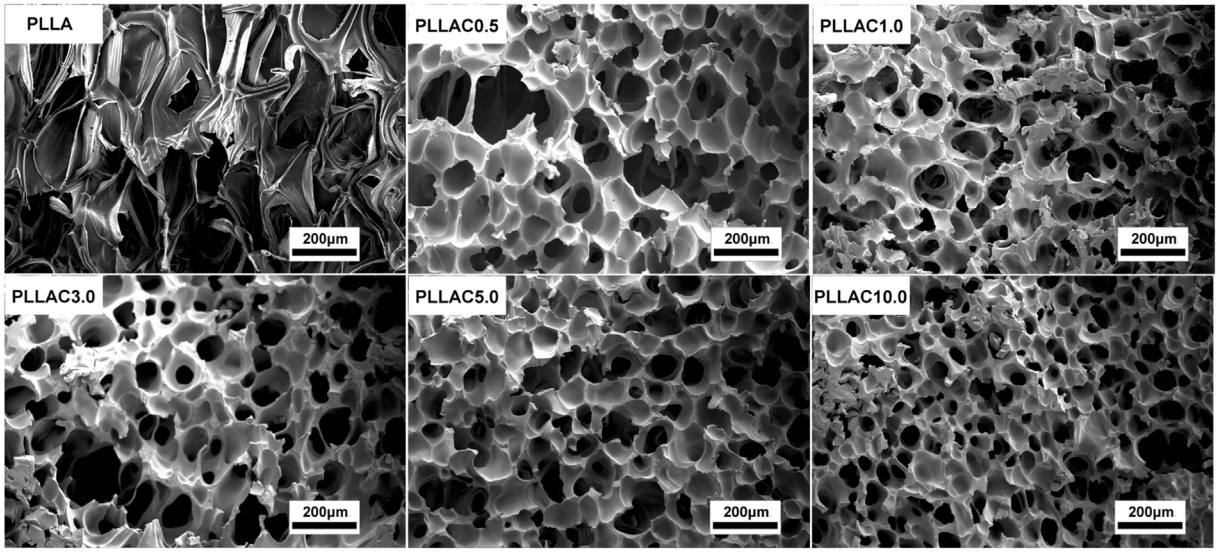

Fig. 4. Foam morphology of PLLA/MWCNT nanocomposites as a function of MWCNT content.

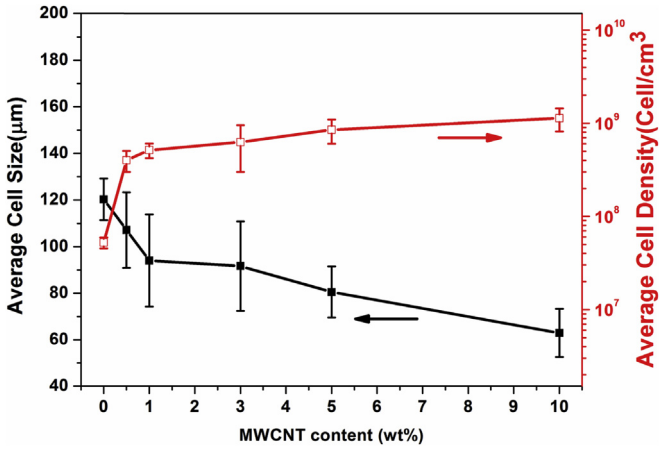

Fig. 5. Average pore size and density of PLLA and PLLA-MWCNT nanocomposite foams saturated at 140 °C, 20 MPa and foamed at 120 °C, 20 MPa. (A color version of this figure can be viewed online.)

conductivity of 0.16 S/m (~5wt% MWCNT) exhibits the EMI SE value of around ~19 dB at the X-band frequency range, which is close to the target EMI SE value for practical application (~20 dB). When the MWCNT loadings reaches 10wt%, the EMI SE value of nanocomposite foams with a conductivity of 3.4 S/m increases up to around ~23 dB, exceeding the target value of desired electrical conductivity (1 S/m) and EMI SE (~20 dB) for commercial applications.

More importantly, as first proposed by Gupta et al. [11], the specific EMI SE (divided the EMI SE by density) is considered more suitable for evaluating the EMI shielding abilities of low-density porous materials. The EMI SE of PLLA/MWCNT nanocomposite foams with ~1.0wt% MWCNT loading is 8.0–11.4 dB, and its corresponding specific average EMI SE can reach around ~44 dB/(g/cm^3) in the measured frequency range. This value is significantly higher than those of typical metals (~10 dB/(g/cm^3)) and other composite foams containing 5wt% graphene. The maximum average specific EMI SE of the PLLA/MWCNT nanocomposite foams (10 wt%) can reach ~77 dB/(g/cm^3) (21.0–24.6 dB), which is the highest value

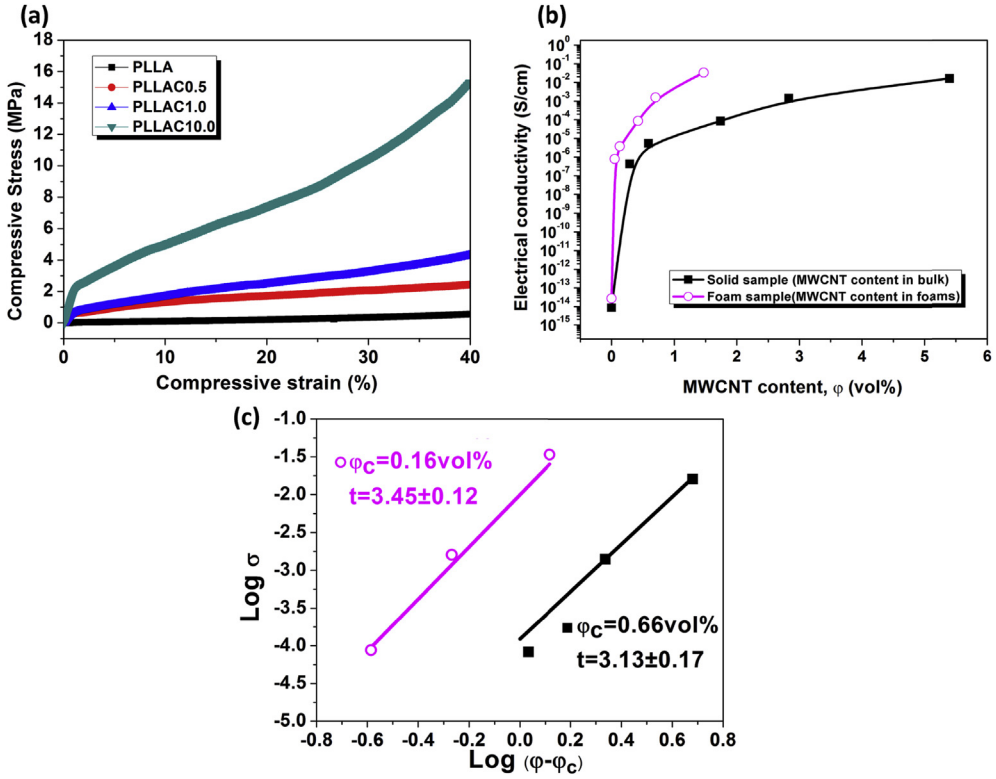

Fig. 6. PLLA/MWCNT nanocomposites and foams as a function of MWCNT content: (a) Compressive stress–strain curves; (b) Electrical conductivity; (c) Power law fitting of the electrical conductivity data from (b). (A color version of this figure can be viewed online.)

MWCNT conductive network in composite foams, thereby providing a fast electron transport channel internally [1].

3.5. EMI shielding of PLLA/MWCNT nanocomposites foams

Fig. 7a shows the EMI SE values of the PLLA/MWCNT composite foams examined in the frequency range of 8.00–12.48 GHz. It is observed that the shielding effectiveness of composites foams exhibits weak frequency dependence in the measured range, but gradually increases with increasing loading of MWCNT in the same frequency range. The PLLA/MWCNT composites foam with a ever reported for MWCNT-based EMI shielding materials and even higher value than many electric fillers-based one at such low-density (0.3 g/cm^3) and thin thickness (2.5 mm) (Table 2).

We also analyzed the EMI shielding mechanism of the PLLA/MWCNT nanocomposite foams. It is well-known that the total EMI shielding effectiveness (SE_{total}) is the sum of the effectiveness of all dissipation, including the absorption of electromagnetic (SE_A), reflection from the surface of materials (SE_A), and multiple reflections in the internal of materials (SE_m) effectiveness (generally ignored when SE_{total} > 15 dB). Fig. 7b shows SE_{total}, SE_A, and SE_R of the PLLA/MWCNT foam composites as a function of MWCNT

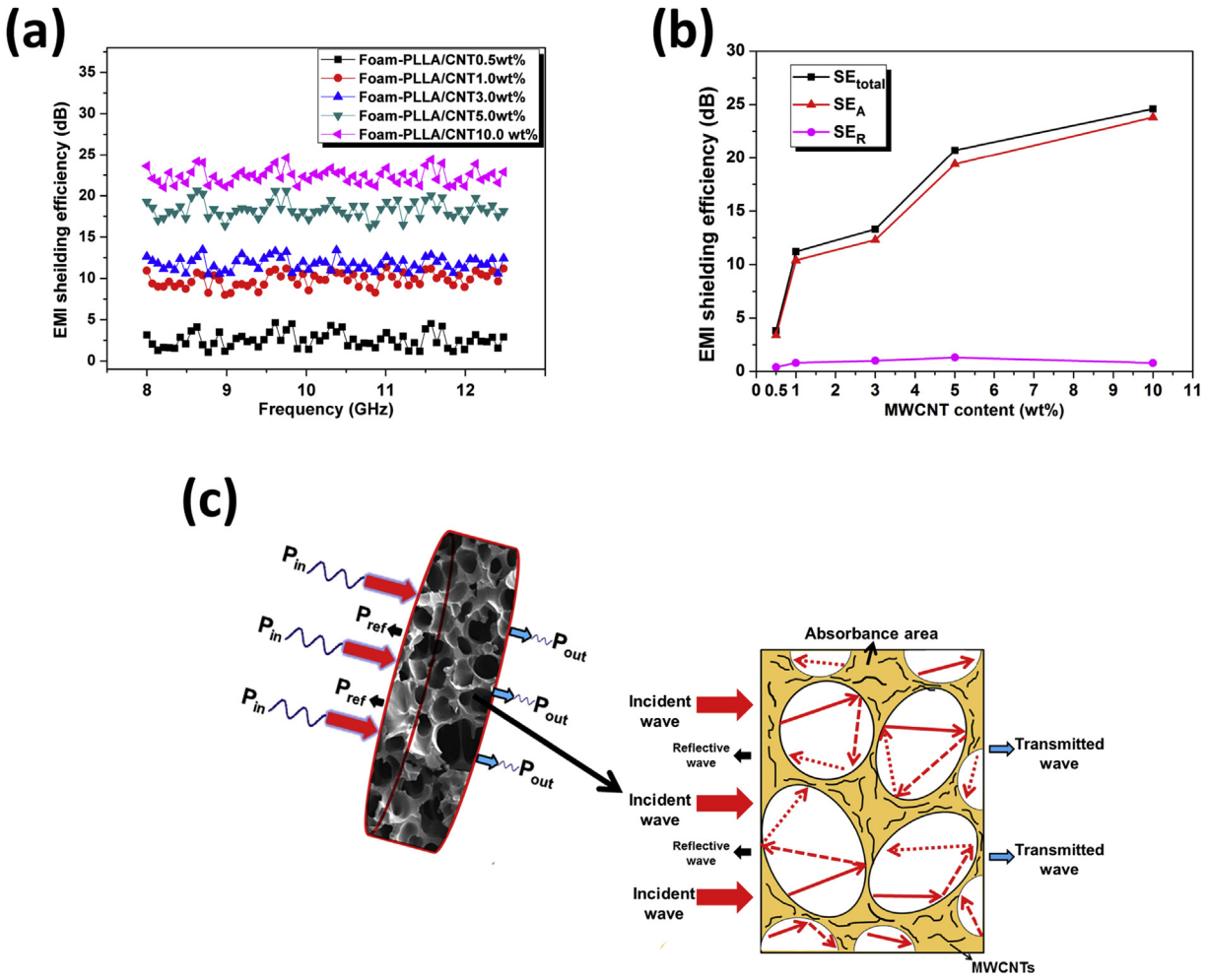

Fig. 7. (a) EMI shielding effectiveness of PLLA/MWCNT foam composites with different MWCNT content measured in the frequency ranges of 8.00–12.48 GHz; (b) SE_{total}, SE_R, and SE_A of PLLA/MWCNT nanocomposites foams at a frequency of 9.75 GHz; (c) Schematic description of electromagnetic microwave dissipation in the PLLA/MWCNT composite foams. (A color version of this figure can be viewed online.)

Table 2
EMI SE of various composite foams measured in the X-band frequency range.

Materials	Type of filler	Filler content	Thickness (mm)	EMI SE (dB)	Specific EMI SE (dB/(g/cm^3))	Specific EMI SE divided by thickness (dB/(g/cm^3)/mm)	Reference
PLLA	MWCNT	10wt%	2.5	23	77	30.8	**This work**
PCL	MWCNT	2wt%	20.0	60–80	193–258	9.7–12.9	[17]
PS	CNTs	7wt%	N/A	19	33.1	N/A	[11]
Cellulose	CNTs	10wt%	2.5	21	219	87.6	[6]
Fluorocarbon	MWCNT	12wt%	3.8	42–48	50–57	13.2–15.0	[31]
PDMS	graphene	0.8wt%	1.0	20	333	333	[1]
PS	graphene	30wt%	2.5	29	64.4	25.7	[4]
PEI	graphene	10wt%	2.3	13	44	19.2	[12]
PMMA	graphene	5wt%	2.4	19	24	10.0	[14]
PVDF	graphene	7wt%	N/A	28	N/A	N/A	[32]
PS	CNF	15wt%	N/A	19	33	N/A	[33]
PP	Carbon fiber	10vol%	3.1	25	34	10.9	[34]
PP	Stainless-steel fiber	1.1vol%	3.1	48	75	24.2	[13]

N/A: not available.

content at 9.75 GHz. As the increase of MWCNT content, both the SE_{total} and SE_A increase while SE_R remains roughly the same (below 1.3 dB). For instance, for the composite foams with a density of 0.3 g/cm^3 and conductivity of 3.4 S/m (~10wt% MWCNT), SE_{total}, SE_A, and SE_R are 24.6, 23.8, and 0.8 dB, respectively, suggesting the contribution of absorption to the EMI SE is much higher than that of reflection in this case. Furthermore, we can get the absorptivity (A), reflectivity (R), and transmissivity (T) coefficients by the equations

(2)–(4). In this work, for the PLLA/MWCNT composite foams with 10wt% MWCNT loadings, the A, R, and T are 0.829, 0.168 and 0.003 at 9.75 GHz, respectively. These results indicate that the primary EMI shielding mechanism of PLLA/MWCNT composite foams systems is absorption rather than reflection in the measured X-band frequency range. The schematic description of electromagnetic microwave dissipation in the PLLA/MWCNT composite foams is shown in Fig. 7c. The incident electromagnetic microwaves can easily enter into the foam composites with less reflection of materials surface due to the highly open-cell structure. Typically, once the incident electromagnetic microwaves contacts the cell, multiple reflections between cell and cell, as well as absorption make it difficult to escape from the absorbance area before being absorbed and dissipated as heat [30]. When added more MWCNTs contents into the PLLA matrix for Sc–CO_2 foaming, the average cell size gradually decreased and cell density increased (Fig. 4). The smaller cell size and higher cell density can further reduce the distance of MWCNTs to make it higher conductive and provide more multiple reflections space to prevent the microwave escape, as well as the thicker cell wall can also effectively attenuate the microwaves from one cell to another cell.

4. Conclusions

In summary, we develop a facile, efficient, environmental friendly and inexpensive approach (pressure-induced flow technique and solid-state supercritical CO_2 foaming) to produce lightweight high-strength PLLA/MWCNT nanocomposites foams with their excellent electrical conductivity and EMI shielding properties. The composite foams with a density of 0.3 g/cm^3 enables a conductivity of 3.4 S/m (~10wt% MWCNT, ~2.5 mm thickness) and EMI SE of around 23 dB in the 8.00–12.48 GHz regions. Its corresponding average specific EMI SE is as high as ~77 dB/(g/cm^3), which far beyond the values of metals and many carbon-based composites with similar densities and thickness. Moreover, the absorption is the dominant EMI shielding mechanism for the PLLA/MWCNT composite foams. The composite foams exhibit superior compressive stress as well. Our results provide a possibility of utilizing biodegradable polymer nanocomposites foam as a lightweight, high-strength, eco-friendly and high performance EMI shielding material in aircraft, automobiles and packaging applications.

Acknowledgments

The authors acknowledge Prof. L. Lee and Dr. H. Yang of the Ohio State University (USA) for the use of facilities and valuable discussions on electrical conductivity and EMI shielding. The authors are grateful to Dr. S. Jiang of the University Bayreuth (Germany) for the characterization of TEM data. The authors acknowledge the financial support of National Natural Science Foundation of China (NO. 51573063 and 21174044), the Guangdong Natural Science Foundation (NO.S2013020013855), the Guangdong Science and Technology Planning Project (NO. 2014B010104004 and 2013B090600126), Zhejiang Natural Science Foundation (NO.LY15E030005) and National Basic Research Development Program 973 in China (NO. 2012CB025902). T. Kuang would like to acknowledge the Chinese Scholarship Council for their financial support of this study and the Nanoscale Science and Engineering Center for the facilities to enable the author to study at the Ohio State University.

References

[1] Z.P. Chen, C. Xu, C.Q. Ma, W.C. Ren, H.M. Cheng, Lightweight and flexible graphene Foam composites for high-performance electromagnetic interference shielding, Adv. Mater. 25 (2013) 1296–1300.
[2] M.S. Cao, W.L. Song, Z.L. Hou, B. Wen, J. Yuan, The effects of temperature and frequency on the dielectric properties, electromagnetic interference shielding and microwave-absorption of short carbon fiber/silica composites, Carbon 48 (2010) 788–796.
[3] N. Li, Y. Huang, F. Du, X.B. He, X. Lin, H.J. Gao, et al., Electromagnetic interference (EMI) shielding of single-walled carbon nanotube epoxy composites, Nano Lett. 6 (2006) 1141–1145.
[4] D.X. Yan, P.G. Ren, H. Pang, Q. Fu, M.B. Yang, Z.M. Li, Efficient electromagnetic interference shielding of lightweight graphene/polystyrene composite, J. Mater. Chem. 22 (2012) 18772–18774.
[5] S. Maiti, N.K. Shrivastava, S. Suin, B.B. Khatua, Polystyrene/MWCNT/graphite nanoplate nanocomposites: efficient electromagnetic interference shielding material through graphite nanoplate-MWCNT-graphite nanoplate networking, Acs Appl. Mater. Inter. 5 (2013) 4712–4724.
[6] H.D. Huang, C.Y. Liu, D. Zhou, X. Jiang, G.J. Zhong, D.X. Yan, et al., Cellulose composite aerogel for highly efficient electromagnetic interference shielding, J. Mater. Chem. A 3 (2015) 4983–4991.
[7] L.C. Jia, D.X. Yan, C.H. Cui, X. Jiang, X. Ji, Z.M. Li, Electrically conductive and electromagnetic interference shielding of polyethylene composites with devisable carbon nanotube networks, J. Mater. Chem. C 3 (2015) 9369–9378.
[8] N. Yousefi, X.Y. Sun, X.Y. Lin, X. Shen, J.J. Jia, B. Zhang, et al., Highly aligned graphene/polymer nanocomposites with excellent dielectric properties for high-performance electromagnetic interference shielding, Adv. Mater. 26 (2014) 5480–5487.
[9] B. Wen, M.S. Cao, Z.L. Hou, W.L. Song, L. Zhang, M.M. Lu, et al., Temperature dependent microwave attenuation behavior for carbon-nanotube/silica composites, Carbon 65 (2013) 124–139.
[10] M.S. Cao, X.X. Wang, W.Q. Cao, J. Yuan, Ultrathin graphene: electrical properties and highly efficient electromagnetic interference shielding, J. Mater. Chem. C 3 (2015) 6589–6599.
[11] Y.L. Yang, M.C. Gupta, Novel carbon nanotube-polystyrene foam composites for electromagnetic interference shielding, Nano Lett. 5 (2005) 2131–2134.
[12] J.Q. Ling, W.T. Zhai, W.W. Feng, B. Shen, J.F. Zhang, W.G. Zheng, Facile preparation of lightweight microcellular polyetherimide/graphene composite foams for electromagnetic interference shielding, Acs Appl. Mater. Inter. 5 (2013) 2677–2684.
[13] A. Ameli, M. Nofar, S. Wang, C.B. Park, Lightweight polypropylene/stainless-steel fiber composite foams with low percolation for efficient electromagnetic interference shielding, Acs Appl. Mater. Inter. 6 (2014) 11091–11100.
[14] H.B. Zhang, Q. Yan, W.G. Zheng, Z.X. He, Z.Z. Yu, Tough graphene-polymer microcellular foams for electromagnetic interference shielding, Acs Appl. Mater. Inter. 3 (2011) 918–924.
[15] L. Monnereau, L. Urbanczyk, J.M. Thomassin, T. Pardoen, C. Bailly, I. Huynen, et al., Gradient foaming of polycarbonate/carbon nanotube based nanocomposites with supercritical carbon dioxide and their EMI shielding performances, Polymer 59 (2015) 117–123.
[16] S. Frackowiak, J. Ludwiczak, K. Leluk, K. Orzechowski, M. Kozlowski, Foamed poly(lactic acid) composites with carbonaceous fillers for electromagnetic shielding, Mater. Des. 65 (2015) 749–756.
[17] J.M. Thomassin, C. Pagnoulle, L. Bednarz, I. Huynen, R. Jerome, C. Detrembleur, Foams of polycaprolactone/MWNT nanocomposites for efficient EMI reduction, J. Mater. Chem. 18 (2008) 792–796.
[18] M. Nofar, C.B. Park, Poly (lactic acid) foaming, Prog. Polym. Sci. 39 (2014) 1721–1741.
[19] D.C. Li, D.J. Fu, Y.C. Yen, A. Benatar, X.F. Peng, D.Y. Chiu, et al., Ultrasound-assisted-pressure-induced-flow leading to superior polymer/carbon nanotube composites and foams, Polymer 80 (2015) 237–244.
[20] Y. Li, B. Shen, X. Pei, Y. Zhang, D. Yi, W. Zhai, et al., Ultrathin carbon foams for effective electromagnetic interference shielding, Carbon 100 (2016) 375–385.
[21] W.Y. Huang, X.L. Ouyang, L.J. Lee, High-performance nanopapers based on benzenesulfonic functionalized graphenes, Acs Nano 6 (2012) 10178–10185.
[22] X.L. Ouyang, W.Y. Huang, E. Cabrera, J. Castro, L.J. Lee, Graphene-graphene oxide-graphene hybrid nanopapers with superior mechanical, gas barrier and electrical properties, Aip Adv. 5 (2015) 017135.
[23] Y. Gao, L.Q. Liu, Z. Zhang, Mechanical performance of nano-CaCO3 filled polystyrene composites, Acta Mech. Solida Sin. 22 (2009) 555–562.
[24] W.T. Zhai, J. Yu, L.C. Wu, W.M. Ma, J.S. He, Heterogeneous nucleation uniformizing cell size distribution in microcellular nanocomposites foams, Polymer 47 (2006) 7580–7589.
[25] G.H. Yang, J.J. Su, J. Gao, X. Hu, C.Z. Geng, Q. Fu, Fabrication of well-controlled porous foams of graphene oxide modified poly(propylene-carbonate) using supercritical carbon dioxide and its potential tissue engineering applications, J. Supercrit. Fluid 73 (2013) 1–9.
[26] A.J. Svagan, M.A.S.A. Samir, L.A. Berglund, Biomimetic foams of high mechanical performance based on nanostructured cell walls reinforced by native cellulose nanofibrils, Adv. Mater. 20 (2008) 1263–1269.
[27] C. Delabarde, C.J.G. Plummer, P.E. Bourban, J.A.E. Manson, Biodegradable polylactide/hydroxyapatite nanocomposite foam scaffolds for bone tissue engineering applications, J. Mater. Sci. Mater. M. 23 (2012) 1371–1385.
[28] L. Hu, D.S. Hecht, G. Gruner, Percolation in transparent and conducting carbon nanotube networks, Nano Lett. 4 (2004) 2513–2517.
[29] M.P. Tran, C. Detrembleur, M. Alexandre, C. Jerome, J.M. Thomassin, The influence of foam morphology of multi-walled carbon nanotubes/poly(methyl

methacrylate) nanocomposites on electrical conductivity, Polymer 54 (2013) 3261–3270.
[30] K.J. Ji, H.H. Zhao, J. Zhang, J. Chen, Z.D. Dai, Fabrication and electromagnetic interference shielding performance of open-cell foam of a Cu-Ni alloy integrated with CNTs, Appl. Surf. Sci. 311 (2014) 351–356.
[31] A. Fletcher, M.C. Gupta, K.L. Dudley, E. Vedeler, Elastomer foam nanocomposites for electromagnetic dissipation and shielding applications, Compos. Sci. Technol. 70 (2010) 953–958.
[32] V. Eswaraiah, V. Sankaranarayanan, S. Ramaprabhu, Functionalized Graphene-PVDF Foam Composites for EMI Shielding, Macromol. Mater. Eng. 296 (2011) 894–898.
[33] Y.L. Yang, M.C. Gupta, K.L. Dudley, R.W. Lawrence, Conductive carbon nanoriber-polymer foam structures, Adv. Mater. 17 (2005) 1999–2003.
[34] A. Ameli, P.U. Jung, C.B. Park, Electrical properties and electromagnetic interference shielding effectiveness of polypropylene/carbon fiber composite foams, Carbon 60 (2013) 379–391.